JOURNAL OF Materials CHEMISTRY

Chemical bonding and magnetism in the germanides HT-UCo_2Ge_2, UGe_3 and $U_3Co_4Ge_7$ from local spin density functional calculations

S. F. Matar,[a] V. Eyert,[b] S. Najm,[c] B. Chevalier[a] and J. Etourneau[a]

[a] *Institut de Chimie de la Matière Condensée de Bordeaux: ICMCB-CNRS, Château Brivazac, 87, avenue du Docteur Albert Schweitzer, F-33608 Pessac Cedex, France*

[b] *Hahn-Meitner Institut, Glienicker Strasse 100, D-14109 Berlin, Germany*

[c] *The Lebanese University, Faculty of Sciences at Fanaar, Beirut, Lebanon*

The electronic and magnetic structures of HT-UCo_2Ge_2 (high temperature form), UGe_3 and of the new intermetallic system $U_3Co_4Ge_7$ are self-consistently calculated within the local spin density functional theory using the augmented spherical wave (ASW) method. The influence of hybridisation on the chemical bonding and magnetic behaviour is discussed from the densities of states (DOS) as well as from the crystal orbital overlap population (COOP) which was recently combined with the ASW method. From this we address the modifications of both chemical bonding characteristics and of magnetic polarisations of uranium and cobalt in HT-UCo_2Ge_2 and UGe_3, these two compounds being considered as the building blocks of $U_3Co_4Ge_7$.

Introduction

Uranium ternary intermetallic systems, $U_xT_yX_z$ (T = *n*d transition metal and group X = IIIA or IVA element), have been widely investigated in the past two decades both experimentally and theoretically because of the large variety of electronic and magnetic properties they exhibit.[1–4] This diversity is mainly due to the interplay of mechanisms promoting magnetism and hybridisation effects of the different constituents in the crystal lattice. Besides structural factors, the mechanism of intra-band spin polarisation in uranium intermetallic systems is based on the interactions within the uranium sublattice as well as on the hybridisation of uranium states with those of the respective transition metal and X elements, 5f–d and 5f–p. The interaction between uranium atoms in the lattice depends on the so-called Hill critical distance, $d_{U-U} = 3.5$ Å. Generally below this value there is no intra-band spin polarisation because the U 5f bands broaden due to the direct overlap between them. The hybridisation of uranium orbitals and those of the transition metal neighbours depends on two main factors involving the distance between uranium and the transition metal and the details of the crystal structure.

This work is part of a systematic study of uranium intermetallic systems prepared and characterised at the ICMCB-CNRS,[4–5] the last one of which is concerned with a detailed study of uranium UT_2Ge_2 germanides for the T = 3d transition metals. These germanides crystallise in the well known $ThCr_2Si_2$-type structure but for T = Co another crystal form exists. It is referred to as the high temperature form, HT-UCo_2Ge_2, in contrast to the labelling of the intermetallic belonging to the formerly studied series as the low temperature (LT) form. The interest in HT-UCo_2Ge_2 arises from its occurrence as one of the building blocks in the recently evidenced $U_3Co_4Ge_7$ intermetallic system,[6] the other building blocks being Cu_3Au-type UGe_3 motifs. HT-UCo_2Ge_2 and UGe_3 are respectively a paramagnet down to 1.7 K and a Pauli paramagnet. For $U_3Co_4Ge_7$, preliminary investigations of magnetic measurements point to a ferromagnetic order at 21.5 K but the magnetic phase diagram seems to be a complicated one[6] so that neutron diffraction investigations are duly planned to determine it. From these observations, the purpose of this work is to investigate the electronic structures and the chemical bonding characteristics of the three uranium-based systems and to assess the changes in chemical bonding which occur when we move from the building blocks HT-UCo_2Ge_2 and UGe_3 to the compound formed by them, $U_3Co_4Ge_7$.

Method of calculation

Our investigations are based on *ab initio* electronic structure calculations derived from spin polarised density functional theory (DFT) in its local density approximation (LDA). We use the LDA parametrization scheme of von Barth and Hedin[7] and Janak.[8] In particular we have applied the augmented spherical wave (ASW) method[9] in a scalar relativistic implementation.[10] In these calculations uranium 5f states were part of the set of valence states. For the different species present, this set was as follows: U: 7s, 7p, 6d, 5f; T: 4s, 4p, 3d; Ge: 4s, 4p, 4d. Energetically low lying Ge($3d^{10}$) states were considered as core states. Using the atomic sphere approximation (ASA), the ASW method assumes overlapping spheres centred on the atomic sites; the volume of all spheres is equal to the cell volume. This is unproblematic for compact structures such as that of the intermetallic systems. However for poorly packed crystal structures such as the Cu_3Au-type of UGe_3, the empty space (body center interstitial site) is represented by pseudo-atoms with $Z = 0$ called empty spheres (ES), whose introduction is necessary to avoid a too large overlap between the actual atomic spheres of U and Ge. Within the ASA our choice of the radii was optimized such as to reduce the overlap between the atomic spheres. Self-consistency was achieved using a new algorithm;[11] the criteria being $\Delta Q < 10^{-8}$ and $\Delta E < 10^{-8}$ *R* (Rydberg) respectively for charge transfers and total energy.

Furthermore, the chemical bonding properties will be discussed based on the concept of crystal orbital overlap population (COOP).[12] In short the COOP is based on the expectation values of operators which consist of the non-diagonal elements of the overlap population matrix,

$$c^*_{ni}(\boldsymbol{k}) S_{ij} c_{nj}(\boldsymbol{k}) = c^*_{ni}(\boldsymbol{k}) < \chi_{ki}(\boldsymbol{r}) | \chi_{kj}(\boldsymbol{r}) > c_{nj}(\boldsymbol{k})$$

where S_{ij} represents an element of the overlap matrix of the basis functions $\chi_{k\_i,j}$ and the $c_{n\_i,j}(\boldsymbol{k})$ are the expansion coefficients entering the wave function of the *n*th band. Partial COOP coefficients $C_{ij}(E)$ are then obtained by integrating the above expression over the Brillouin zone:

$$C_{ij}(E) = C_{ji}(E) = 1/\Omega_{BZ} \; \Sigma_n \int_{BZ} d^3\boldsymbol{k} \; \mathrm{Re}\{c^*_{ni}(\boldsymbol{k}) S_{ij} c_{nj}(\boldsymbol{k})\} \delta(E - \varepsilon_{nk})$$

(Ω_{BZ} = volume of the Brillouin zone, δ = Dirac notation delta serving as a counter of states) which in a somewhat lax notation is often designated as the overlap-population-weighted DOS. The total COOP are then evaluated as the sum over all non-diagonal elements, *i.e.*

$$C(E) = \Sigma_{ij\ (i \neq j)}\ C_{ji}(E)$$

For a detailed description and for significant examples we refer the reader to a recent work by one of us.[13] Recently we implemented the COOP in the ASW method with the objective to extract further information on the chemical bonding. This enabled the calculation of the COOP within density functional theory.

Crystal structures

The unit cell of $U_3Co_4Ge_7$ is sketched in Fig. 1(a). It consists of an elongated body centered tetragonal (bct) lattice (space group *I*4/*mmm*; $Z = 2$) with a small a lattice constant (a = 4.109 Å) and a large c/a ratio of 6.6875.[6] The view can be made easier to understand if one considers the building blocks shown in Fig. 1(b) and (c). Therefore we start by describing the other two structures and turn back to that of $U_3Co_4Ge_7$ at the end of this section.

Whereas the structure of UGe_3 is readily visualised as a primitive cubic lattice of Cu_3Au-type (space group *Pm*3*m*, $Z = 1$) shown in Fig. 1(b), the structure of HT-UCo_2Ge_2 can be further understood when compared with the low temperature (LT) form. The LT and HT structures are shown in Fig. 1(c). The LT form is the well known bct $ThCr_2Si_2$-type structure (space group *I*4/*mmm*, $Z = 2$) where U(Th) is surrounded by 8 Co(Cr) and 8 Ge(Si) atoms giving independently two kinds of square prisms twisted by 45° with respect to each other. Perpendicular to the c-axis, U atoms form planes at z = 0 and $z = 1/2$ which are interlayered by planes containing Co ($z = 1/4$ and 3/4) and Ge ($z = \pm 0.375$ and ± 0.125) atoms respectively. Hence the structure can be described as a succession of $\{Co_2Ge_2\}$ double layers perpendicular to the c-axis with the sequence U-(Co_2Ge_2)-U-(Co_2Ge_2). The HT-UCo_2Ge_2 structure is derived from the $CaBe_2Ge_2$-type structure which shows a certain similarity to the formerly described $ThCr_2Si_2$ structure. The succession of $\{Co_2Ge_2\}$ double layers is still present but Co(Be) and Ge positions are interchanged in one layer. This causes a breaking of translation symmetry and a simple tetragonal Bravais lattice is obtained. There are then two types of site for each transition metal, Co_1 and Co_2, and for the X element, Ge_1 and Ge_2. Both types of transition metal atoms form squares lying perpendicular to the c axis which are rotated by 45° relative to each other. This should affect the type of d orbitals stabilised by the tetrahedral-like crystal field of surrounding Ge atoms as will be discussed in the following sections. Turning to U(Ca), it now becomes surrounded by four atoms of each sort forming two interpenetrating but not independently constituted square prisms.

Whereas the room temperature a lattice constants of the LT-UCo_2Ge_2 and HT-UCo_2Ge_2 forms are close, the c/a ratios are 2.455 and 2.324 respectively leading to a smaller unit cell volume for the HT form. This unusual result for a high temperature form should be related to a change of the crystal structure. In the HT form the positions of Co and Ge in subsequent Co_2Ge_2 layers are interchanged, allowing for a closer packing of the crystal structure. As a consequence, the underlying Bravais lattice is simple tetragonal rather than body-centered tetragonal. Arguments based on the magnetic order do not hold here, since the LT form is an antiferromagnet only at 175 K leading to a large c/a ratio, whereas the HT form is a paramagnet down to 1.7 K.

From the above description we find in $U_3Co_4Ge_7$ [Fig. 1(a)] two uranium sublattices: one UGe_3 related and the other HT-UCo_2Ge_2 related, referred to as U_1 and U_2 respectively. The two cobalt sublattices are labelled as in the HT-UCo_2Ge_2 compound. The three Ge sublattices are one UGe_3 related and two HT-UCo_2Ge_2 related, referred to as Ge_1, Ge_2 and Ge_3 respectively.

This is however a schematic description of the structure because when the $U_3Co_4Ge_7$ intermetallic is formed, atoms

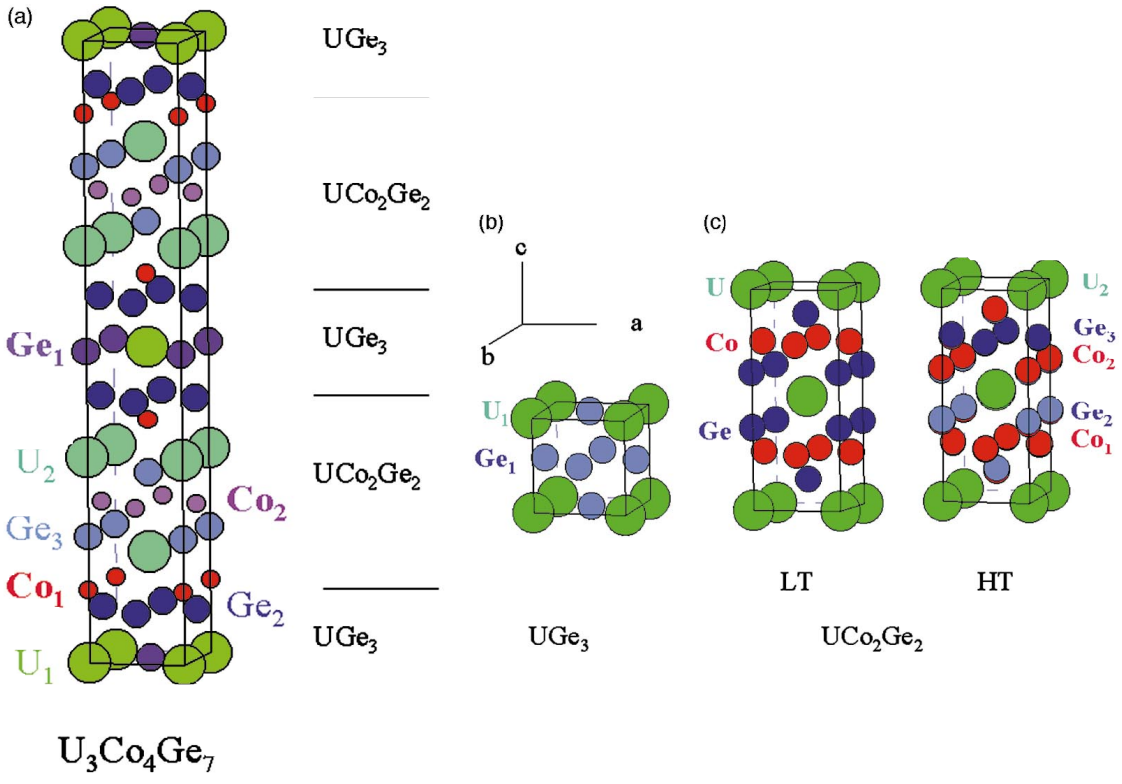

Fig. 1 Crystal structures of $U_3Co_4Ge_7$ (a), UGe_3 (b), and UCo_2Ge_2 (c) in its low temperature (LT) and high temperature (HT) forms. The labelling of the atoms in UGe_3 and HT-UCo_2Ge_2 is similar to the labelling in $U_3Co_4Ge_7$.

formerly belonging to the building blocks become shared in the new structure and mixing between the relevant states will show different behaviours when compared with UGe_3 and UCo_2Ge_2 as we shall discuss in the following sections.

The lattice constants used throughout the calculations are obtained from experimental investigations whose crystallographic results are collected together in ref. 6.

Results

Non-magnetic calculations

Objectives of the non-magnetic calculations. As a first part of this work calculations were performed assuming non-magnetic ground states; *i.e.* we enforced spin degeneracy for all states. From the results of such non-spin polarised (NSP) calculations the chemical bonding can be easily addressed. This is related to the fact that the spin polarised bands, to first order, result from the NSP bands by a rigid band shift. Hence it is justified to discuss the chemical bonding from the NSP results. Using the Stoner theory of band ferromagnetism, the NSP calculations finally point to the possible onset of magnetism *via* the DOS at the Fermi level.

General remark on the electronic configurations. In the ASA, charge transfers are not a relevant issue in as far as they depend on the choice of the atomic sphere radii which is not unique. In our calculations only small charge transfer could be observed between the different constituents and we do not comment on it. In UGe_3 where an empty sphere was introduced at the body center [Fig. 1(b)], we find that the ES receive a small amount of charge (0.3 electrons) drained from U and Ge. The overall change of electron configurations in all systems points to a typically metallic bonding mechanism, based on the hybridisation between the different states as we have shown before for uranium intermetallic systems of different compositions.[14,15]

Density of states and crystal orbital overlap populations. *General.* In all representations the site projected DOS are shown for the total number of atoms of each class in the unit cell. The energy scale along the horizontal axis is taken with reference to E_F. All plots are given in a narrow energy window $\{-8, +8\ \text{eV}\}$ around E_F to allow for comparison. The partial DOS are shifted with respect to each other along the *y*-axis to make the presentation clear.

The COOP are plotted for interactions between one of each two atomic species. When inter-atomic interactions between two identical species are considered, this refers to Bloch sums of the respective states. The corresponding COOP do not contain the single term which would describe the interaction of a certain orbital with itself. Positive and negative contributions indicate bonding and antibonding states, respectively. When the COOP intensity is low non-bonding interactions are expected.

UGe_3. Fig. 2 gives the DOS [Fig. 2(a)] and the COOP [Fig. 2(b)] for UGe_3. Uranium states are mainly of 5f character; 6d states can be seen in the broad band below E_F so that they contribute to the chemical bonding. These features are shown by the sharp peak of U 5f above E_F and the low intensity DOS at and below E_F respectively. U 7s states close to E_F are resembled by the DOS around -1 eV. Ge 4p states are dominating between -5 eV and E_F. They exhibit a similar outline to the uranium DOS, thus pointing to a covalent bonding between U and Ge [labelled U_1 and Ge_1 respectively in Fig. 1(b)].

The lower part of the U 5f DOS is crossed by the Fermi energy at a low intensity DOS $n(E_F)$. This agrees with the Pauli paramagnetic character of UGe_3 as will be shown

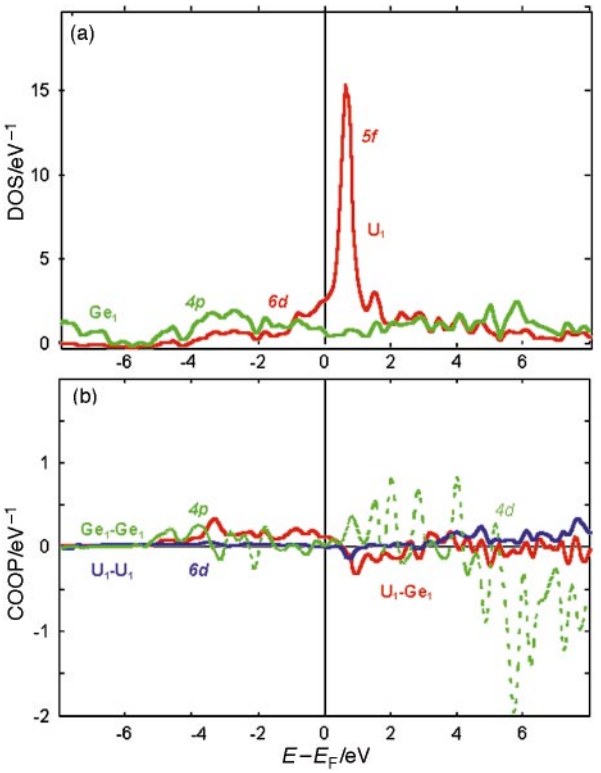

Fig. 2 UGe_3: site projected DOS (a) and COOP of pairwise interactions (b)

throughout the analysis of the NSP DOS in the framework of the Stoner theory of band ferromagnetism and from the results of spin polarised calculations. The presence of the major part of U 5f above E_F corresponds to the low filling (3 out of the 14 quantum f states) of the 5f subshell with roughly 2.9 electrons which is close to the atomic configuration.

Further information can be obtained from the analysis of the COOP for pair interactions. From Fig. 2(b) the U–Ge interactions are predominating in the valence band because they show bonding behaviour throughout whereas the U–U interaction shows little bonding features. Ge–Ge interactions are not negligible around -4 eV but bonding COOP are accompanied by anti-bonding COOP in the valence band. Moreover they show little bonding in the neighbourhood of E_F. Hence one cannot expect them to dominate over the U–Ge interactions. The large intensity modulation of the Ge–Ge COOP in the conduction band arises from empty Ge(4d) states so they are not relevant to the bonding. From this analysis bonding within UGe_3 is dominated by U–Ge interactions which mainly involve U 7s, 6d and Ge 4p, and to lesser extent by Ge–Ge ones in the lower energy parts of 4p orbitals.

HT-UCo_2Ge_2. As described in the crystal structure part, HT-UCo_2Ge_2 has a simple tetragonal structure with two Co and Ge sublattices. They are labelled after Fig. 1(c) and their closest distances: Co_1–Ge_2 and Co_2–Ge_3; the latter pair of atoms occupy half of the initial Co and Ge sites in the LT form whereas the atoms belonging to the former pair formed of Co_1 and Ge_2 respectively occupy the other half of the Ge and Co positions in the LT form. From this one can understand the differences of the respective DOS in Fig. 3(a). As expected Co_1, Ge_2 and Co_2, Ge_3 show similar DOS thus pointing to the covalent interactions between them. Major differences appear for Co 3d DOS between -3 and -1 eV which show broader features for Co_1 than for Co_2. The overall Co_1 DOS have large similarities with those of LT-UCo_2Ge_2, shown as an inset in Fig. 3(a). The reduced width of the Co_2 DOS points

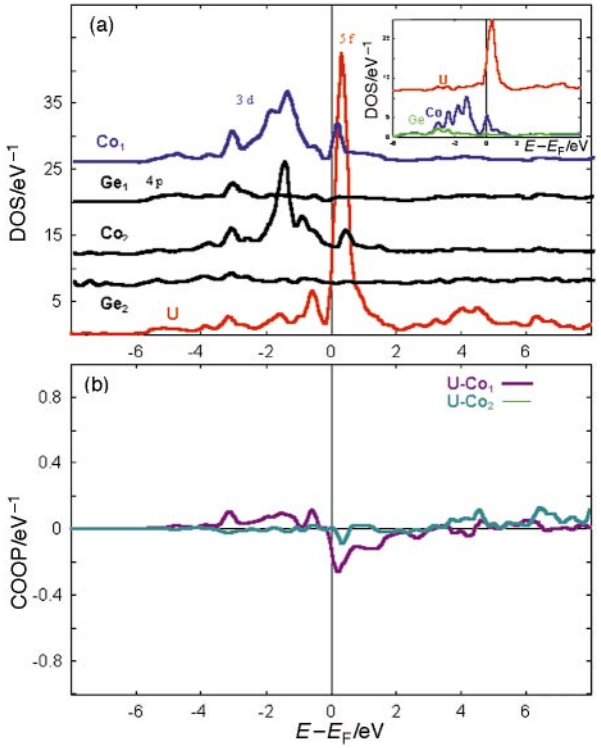

Fig. 3 HT-UCo_2Ge_2: (a) site projected DOS, insert shows the site projected DOS in the LT form; (b) COOP for pairwise interactions between uranium and the two cobalt sublattices

to a lesser mixing with uranium states. This is observed from the plot of the COOP for U–Co interactions given in Fig. 3(b). In the following, U refers to U_2 atoms in Fig. 1(c) (HT). Clearly the U–Co_1 interactions are bonding all over the valence band and become slightly antibonding at E_F whereas U–Co_2 are approximately non-bonding throughout. The attribution of the different features appearing in the COOP such as the peak at -0.5 eV [which will be attributed to d_{z^2} orbitals in Fig. 4(d)] can be achieved from the decomposition of the 5 d orbitals of Co carried out in the following section.

Further, important differences appear around E_F. Just like in UGe_3 the lower part of the U 5f DOS is crossed by the Fermi level but at a slightly larger DOS intensity. This could be in relation to the mixing of U 5f with Co now present in the lattice, whereby the U–Ge distance which is 5.62 a_0 (1 a_0 = 1 Bohr radius = 0.529 Å) in UGe_3 becomes larger in the Co compounds and ranges from 5.79–5.82 a_0 in the HT form to 5.86 a_0 in the LT form. In HT-UCo_2Ge_2 Co_1 is within a tetrahedral environment of Ge which splits the d states into e and t_2 manifolds, the latter being split further by the T_d-like crystal field. Whereas the former comprises of $d_{x^2-y^2}$ and d_{z^2}, the latter is made from d_{xy}, d_{xz} and d_{yz}. The projection of the Co d DOS over the 5 d orbitals is shown in Fig. 4. The e-like orbitals derive from d_{xy} and d_{z^2} for Co_1 and $d_{x^2-y^2}$ and d_{z^2} for Co_2 due to the 45° rotation between the two positions and to the resulting square-pyramid-like environment of Co_2. From Fig. 4(a) and (b) the two cobalt sublattices exhibit different behaviour for the in-plane orbitals. Consequently the Co_1 DOS at E_F, $n(E_F)$, are mainly due to d_{xy} orbitals and to a lesser extent to d_{z^2} orbitals Fig. 4(d) and the purely Co_2 d DOS at 0.5 eV is due to $d_{x^2-y^2}$. These states are likely to mix with U 5f close to E_F whereas the lower energy parts are involved with Co–Co bonding around –2 eV and Co–Ge below -4 eV. The relatively large Co_1 $n(E_F)$ is related to the possible onset of a local magnetic moment. Moreover this points to a larger magnetic moment on Co_1 as with respect to Co_2 which shows vanishing DOS at E_F. Lastly it can be noticed that rather similar behaviour is observed for out-of-plane d_{xz} and d_{yz} orbitals, as can be observed from Fig. 4(c).

$U_3Co_4Ge_7$. The site projected DOS for uranium ($1U_1$, $2U_2$) and cobalt ($2Co_1$, $2Co_2$) sites in $U_3Co_4Ge_7$ are given in Fig. 5(a); those of Ge sites are discarded to make the presentation clear. Just like in the formerly studied compounds, E_F crosses the lower part of the uranium 5f states but at a larger $n(E_F)$ for U_2 than for U_1 on the one hand and with a larger U_2 $n(E_F)$ than in HT-UCo_2Ge_2 on the other hand. Whereas this is in accordance with the fact that of U_2 belongs to the group of UCo_2Ge_2 related building blocks, and U_1 to UGe_3 ones, the larger U_2 $n(E_F)$ arises from a larger mixing between uranium and cobalt due to the shorter U_2–Co_1 distance in $U_3Co_4Ge_7$ (5.69 a_0) than in UCo_2Ge_2 ($d_{U-Co_1} = 5.88$ a_0). The quantitative analysis of the respective $n(E_F)$ values will be carried out in the following section. The mixing between the uranium states with those of both cobalt sites can be observed in the valence band from the resemblance of the DOS in the energy range {-4, 0 eV}; below -4 eV one expects mixing with Ge states. The analysis of the cobalt DOS follows from that of the previous section dealing with HT-UCo_2Ge_2.

At this point more information on the chemical bonding can be obtained from the discussion of the COOP within $U_3Co_4Ge_7$. Fig. 5(b) gives the pairwise interactions between the different uranium and cobalt sites. Clearly the predominating interaction is between U_2 and Co_1 whose COOP are very similar to those of U–Co_1 in HT-UCo_2Ge_2. The larger COOP intensity at E_F agrees with the larger U_2 $n(E_F)$. Thus the predominating interaction in the bonding between U and Co sublattices can be assigned to the U_2–Co_1 bond.

We now discuss the other interactions within the lattice without showing the COOP curves. Between U and Ge we find the strongest interactions to occur within the UGe_3 related motif, *i.e.* for the U_1–Ge_1 interaction and to a lesser extent for the U_1–Ge_2 one. Little role can be assigned to the U_1–Ge_3 interaction because Ge_3 is mostly involved with the bonding within the UCo_2Ge_2 building block [Fig. 1(a)]. For the same reasons the U_2–Ge interactions play little role. Like the other U–Ge interactions it is found to be bonding throughout the valence band. From this the stability of the structure regarding U–Ge interactions is ensured by the U_1 sublattice interacting with Ge_1 as well as with Ge_2 sublattices. Lastly we comment on the Co–Ge interactions. They are found to occur through the Ge_3 sublattice as one may expect from the discussion in the preceding paragraph.

Analysis of the NSP-DOS within the Stoner theory. In as far as U 5f as well as Co 3d states were treated as band states in the framework of our calculations, the Stoner theory of band ferromagnetism can be applied to give a first impression of the features of spin polarisation of collective electrons for these bands. At zero temperature the product $In(E_F)$ provides a criterion for the instability of the non-magnetic configuration (equal occupation of the two spin states) towards spin-polarisation (unequal spin occupation) if $In(E_F) > 1$. The system then stabilises through a gain of energy due to exchange. Here I is the Stoner exchange-correlation integral which is an atomic quantity that can be derived from spin-polarised calculations[16] and $n(E_F)$ the DOS at E_F in the non-magnetic state. I{U(5f)} and I{Co(3d)} are found close to 0.035 R (0.45 eV). Table 1 gives the $n(E_F)$ and $In(E_F)$ values for the different atomic sites. All atoms except Co_2 are expected to polarise, *i.e.* to carry magnetic moments. This is somehow in contradiction with experimental observations of Pauli paramagnetic UGe_3 and paramagnetic HT-UCo_2Ge_2.

But one should consider the values of $In(E_F)$ as only indicative for the reasons given above, and that only spin-polarised calculations can allow a magnetic moment to be proven. From this the computed $In(E_F)$ values should help us

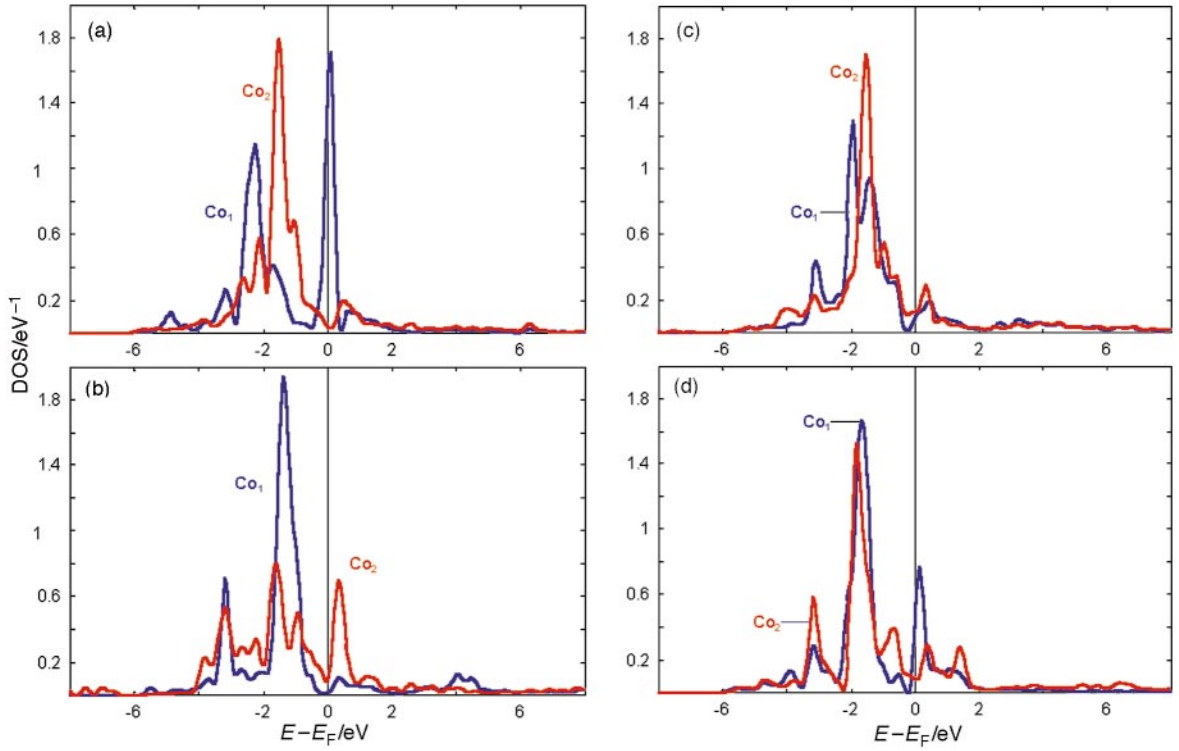

Fig. 4 HT-UCo_2Ge_2. Crystal field components for d orbitals of cobalt: (a) d_{xy}, (b) $d_{x^2-y^2}$, (c) d_{xz} and d_{yz}, (d) d_{z^2}.

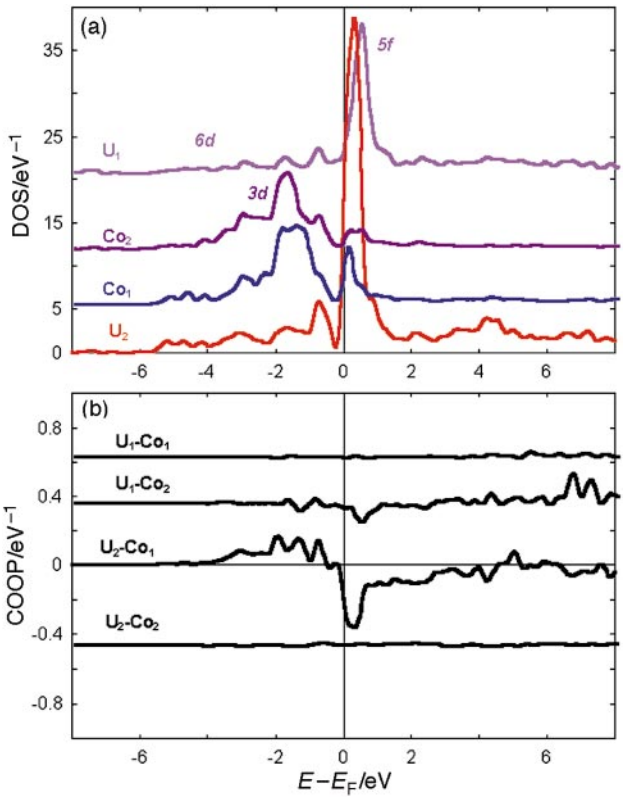

Fig. 5 Non-magnetic calculations of $U_3Co_4Ge_7$: (a) site projected DOS for U and Co sublattices, (b) COOP for the different U–Co interactions

to point towards a tendency for larger and larger spin polarisation within the series under investigation, *i.e.* from UGe_3 to HT-UCo_2Ge_2 to $U_3Co_4Ge_7$. With these observations in mind, three relevant results can be found from the trends in Table 1: (i) that the presence of the UGe_3 building block-related U_1 atom within $U_3Co_4Ge_7$ increases its magnetic polarisation; (ii) that the presence of HT-UCo_2Ge_2-related U_2 within $U_3Co_4Ge_7$ increases its magnetic polarisation. Moreover it should carry a much larger magnetic moment than U_1; (iii) that the ability of Co_1 to carry a magnetic moment of its own increases from HT-UCo_2Ge_2 to $U_3Co_4Ge_7$. This is also observed for Co_2 whose $In(E_F)$ value becomes twice as large but remains below the Stoner criterion.

Spin polarised (SP) calculations

Spin polarised (SP) calculations were then carried out for the three systems. This was done by initially allowing for two spin occupations for all atomic species then self-consistently converging the charges and the magnetic moments. We carried out spin only ferromagnetic calculations despite the large orbital moments μ_L on uranium in such systems.[4,17] Orbital moments are of opposite sign to spin-only, μ_{SO}, moments (Hund's second rule; remember $5f^3$ occupation of uranium) and with magnitudes in the range $1 < -\mu_L/\mu_{SO} < 2.6$, according to the magnitude of hybridization of uranium with its ligands: whereas the upper limit value refers to U^{3+} free ion, strongly hybridized systems such as UT_2 (T = Fe, Co, Ni) have ratios close to 1.[18] Thus accounting for spin–orbit coupling effects becomes compulsory. Our limitation to spin-only calculations is due to the large unit cells involved for $U_3Co_4Ge_7$ and for HT-UCo_2Ge_2 which would involve exceedingly long computation times.

Table 1 NSP DOS at Fermi level and Stoner products for the three germanide systems

	$n(E_F)U_1/R^{-1}$	$n(E_F)U_2/R^{-1}$	$n(E_F)Co_1/R^{-1}$	$n(E_F)Co_2/R^{-1}$	$In(E_F)U_1$	$In(E_F)U_2$	$In(E_F)Co_1$	$In(E_F)Co_2$
UGe_3	37.8				1.3			
HT-UCo_2Ge_2		72.5	29.3	6.4		2.5	1.0	0.2
$U_3Co_4Ge_7$	61.5	127.1	38.5	12.0	2.2	4.4	1.3	0.4

Table 2 Spin only magnetic moments and total magnetisations for the three germanide systems

	M/μ_B (U_1)	M/μ_B (U_2)	M/μ_B (Co_1)	M/μ_B (Co_2)	M/μ_B (total)
UGe_3	0				0
HT-UCo_2Ge_2		−0.045	0.18	0.005	0.28
$U_3Co_4Ge_7$	−0.012 (6d) 0.226 (5f) 0.214	0.068 (6d) 1.478 (5f) 1.546	−0.71	−0.052	$M_{U_1}+2M_{U_2}+2M_{Co_1}+2M_{Co_2}=1.782$

SP calculations for UGe_3 give equal spin populations for the majority (↑) and minority (↓) spins in agreement with the Pauli paramagnetic behaviour of the system. There is no energetical shift between the two spin populations $N(\uparrow)$ and $N(\downarrow)$ which are equal, *i.e.* $N(\uparrow)=N(\downarrow)$ then $M=N(\uparrow)-N(\downarrow)=0$. The calculations for HT-UCo_2Ge_2 result in weak magnitude moments carried by the uranium and cobalt atoms (Table 2). The resulting total moment is very small so that our calculations tend towards the reported paramagnetic behaviour.

Magnetic moments are carried by both uranium sublattices in $U_3Co_4Ge_7$ but with very different magnitudes. This result, which is expected from the Stoner mean field analysis carried out above, is in relation to their belonging to different building blocks in the crystal lattice. From the decomposition of the total moments into 6d and 5f contributions, the major polarization is from U 5f states whereas a small contribution from U 6d states, which amounts to less than 5% of the 5f moment, is observed. We find different magnitudes for the moments carried by cobalt atoms at the two crystallographic sites; their opposite alignment to the moments of uranium points to a likely induced nature. This is contrary to the Stoner criterion discussion above which predicts for Co_1 a magnetic moment of its own (Table 1). This underlines the preliminary character of the Stoner criterion because it mainly refers to atomic quantities whereas the DOS and COOP analyses carried above clearly show the importance of hybridization whereby the strongest interactions between uranium and cobalt sublattices are for the U_2–Co_1 bond. Thus the much larger magnitude of the moment carried by Co_1 is the consequence of its large mixing with U_2. The resulting spin only magnetization per formula unit amounts to 1.78 μ_B. We do not presently have results for low temperature measurements of ordered moments of $U_3Co_4Ge_7$ to compare with. From the discussion of the magnitude of the orbital moment of uranium in the beginning of this section we can estimate the absolute value of the total magnetisation to be close to 0.9 μ_B, if $-\mu_L/\mu_{SO}$ is *ca.* 1.5, *i.e.* halfway between the two extrema. This value should be compared with experimental data when available.

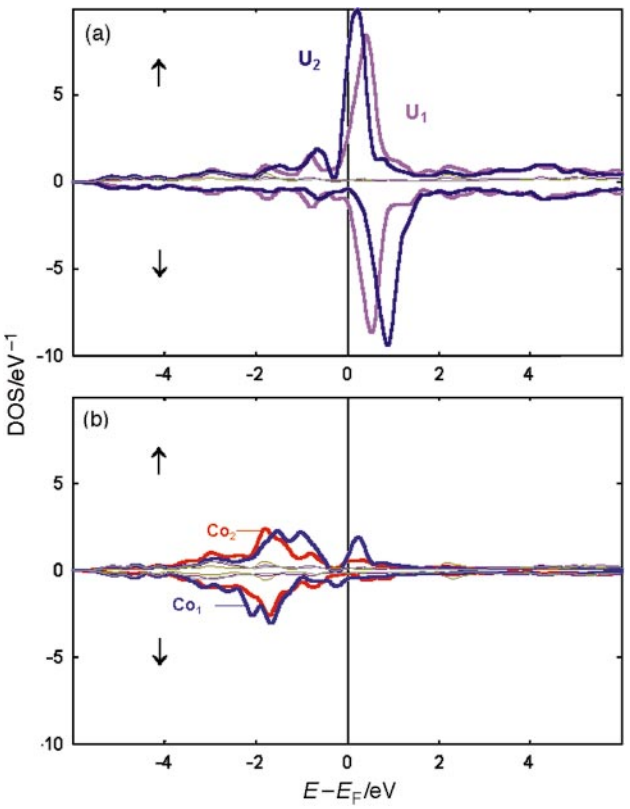

Fig. 6 Spin polarised ferromagnetic calculations for $U_3Co_4Ge_7$: site projected DOS for U (a) and Co (b) sublattices

Fig. 6 shows the site projected DOS in $U_3Co_4Ge_7$ for majority (↑) and minority (↓) spin directions. We concentrate on the effects of spin polarization so that Ge states which do not carry magnetic moments are not discussed here. The very different moments carried by U_1 and U_2 (Table 2) result in different magnitudes of exchange splitting causing the ↑ states to move to lower energy whereas the opposite is observed for ↓ states. A residual large DOS at E_F due to $U_2(\uparrow)$ could be in relation to the large specific heat observed for this compound.[6] For Co_1 which carries a negative sign magnetic moment, a mixing of ↑ states with those of $U_2(\uparrow)$ can be observed, especially where both DOS have the same shape near E_F. This causes them to be shifted upwards in energy. In contrast, minority spin (↓) DOS have the same energetic position as Co_2 for which exchange splitting is small because of lesser mixing with U_2 states.

Conclusion

In this work we have investigated the interplay between hybridisation and magnetism in three germanide systems having structural relationships: HT-UCo_2Ge_2, UGe_3 and the recently prepared intermetallic system $U_3Co_4Ge_7$. Using scalar relativistic calculations and assuming no spin polarisation in the first approach, the trends of the chemical bonding have been examined through the site projected DOS as well as through the COOP. The results of the calculations have allowed the different roles played by the different U, Co and Ge sublattices in $U_3Co_4Ge_7$ to be distinguished through the different binding strengths between them, related to the building blocks HT-UCo_2Ge_2 and UGe_3. Such differences helped the differences of magnitudes and natures of the magnetic moments from the subsequent spin polarised calculations to be addressed. More precise determinations of the magnetic structure of $U_3Co_4Ge_7$ planned in the near future will allow more insight into this new class of ternary uranium germanide system.

Part of the calculations were carried out within the MNI network of intensive numerical calculations pole of the University Bordeaux1. Technical support from the staff of the computer centre of the CRIBx1 is acknowledged.

References

1 Z. Zolnierek and J. Mulak. *J. Magn. Magn. Mater.*, 1995, **140–144**, 1393.
2 M. Kuznietz, H. Pinto, H. Ettedgui and M. Melamud. *Phys. Rev. B*, 1989, **40**, 7328.
3 L. M. Sandratskii and J. Kübler, *Solid State Commun.*, 1994, **91**, 183; *Phys. Rev. B*, 1994, **50**, 5071.
4 S. F. Matar and V. Eyert, *J. Magn. Magn. Mater.*, 1997, **163**, 321;

S. F. Matar, F. Mirambet, B. Chevalier and J. Etourneau, *J. Magn. Magn. Mater*., 1995, **140–144**, 1389; S. F. Matar, *J. Magn. Magn. Mater*., 1995, **151**, 263; S. F. Matar, B. Chevalier and J. Etourneau, *J. Magn. Magn. Mater*., 1994, **137**, 293.
5 S. F. Matar, V. Eyert, A. Mavromaras, S. Najm, B. Chevalier and J. Etourneau, *J. Magn. Mater*., 1997, **174,** 219.
6 R. Pöttgen, B. Chevalier, P. Gravereau, B. Darriet, W. Jeitschko and J. Etourneau, *J. Solid State Chem*., 1995, **115**, 247.
7 J. von Barth and D. Hedin, *J. Phys. C*, 1972, **5**, 1629.
8 J. F. Janak, *Solid State Commun*., 1978, **25**, 53.
9 A. R. Williams, J. Kübler and C. D. Gelatt Jr., *Phys. Rev. B*, 1979, **19**, 6094.
10 D. D. Koelling and B. N. Harmon, *J. Phys. C*, 1977, **10**, 3107.
11 V. Eyert, *J. Comp. Phys*., 1996, **124**, 271.
12 R. Hoffmann, *Angew. Chem., Int. Ed. Engl*., 1987, **26**, 846.
13 V. Eyert, *Density functional methods: Applications in Chemistry and Materials Science*, ed. M. Springborg, Wiley, Chichester, 1997, pp. 233–304.
14 S. F. Matar, V. Eyert, B. Chevalier and J. Etourneau, *Int. J. Quantum Chem*., 1997, **61**, 705.
15 S. F. Matar and V. Eyert, *J. Magn. Magn. Mater*., 1997, **167**, 321.
16 J. F. Janak, *Phys. Rev*., 1977, **16**, 255; V. L. Moruzzi, J. F. Janak and A. R. Williams, *Calculated Electronic Properties of Metals*, Pergamon Press, N.Y., 1978.
17 S. Brooks and B. Johansson, in *Handbook of Magnetic Materials*, ed. K. H. J. Buschow, 1993, 7th edn.
18 B. Lebech, M. Wulff and G. H. Lander, *J. Appl. Phys*., 1991, **69**, 5897.

Paper 7/08736E; *Received* 4*th December*, 1997